Applied Surface Science 608 (2023) 155239

Contents lists available at ScienceDirect

Applied Surface Science

journal homepage: www.elsevier.com/locate/apsusc

Full Length Article

Surface-enhanced Raman spectroscopy for the detection of microplastics

L. Mikac [a,b], I. Rigó [b], L. Himics [b], A. Tolić [a], M. Ivanda [a,*], M. Veres [b,*]

[a] Molecular Physics and New Materials Synthesis Laboratory, Ruđer Bošković Institute, Bijenička 54, Zagreb, Croatia
[b] Department of Applied and Nonlinear Optics, Institute for Solid State Physics and Optics, Wigner Research Centre for Physics, Budapest, Hungary

ARTICLE INFO

Keywords:
SERS
Microplastics
Polystyrene
Polyethylene
Nanoplastics
Colloids

ABSTRACT

Detection of microplastics is still challenging due to limitations of current methods, instrumentation, and particle size. In this work, surface-enhanced Raman spectroscopy (SERS) was used to detect polystyrene (PS, 350 nm) and polyethylene (PE, 1–4 μm) particles in pure water. Gold nanoparticles (Au NPs) of four different sizes were synthesized, characterized, and used as SERS active substrate for microplastic detection. The Au NPs obtained had a spherical shape with diameters of 33.2, 67.5, and 93.7 nm and an elliptical shape with shorter and longer diameters (nanorods) of 23.5 and 35.5 nm, respectively. The optimal conditions (volume ratio of sample to gold colloid, aggregating agent and its concentration) were determined. The efficient and stable SERS signals were observed on the PS microparticles, while the PE signal was difficult to obtain. The developed SERS method allows the detection of polystyrene microparticles at concentrations as low as 6.5 μg mL^{-1}. The described method can be a useful tool for the detection of microplastic pollutants of this particular size.

1. Introduction

Today, plastics are used in almost every field, including construction, transportation, packaging, textiles, consumer products, electronics, various health applications, and industrial machinery. Plastic is the material of choice because it is lightweight, flexible, versatile, hygienic, cost-effective and very durable. Therefore, plastic production has increased dramatically in recent decades [1,2]. Although the benefits of using plastics are numerous, their widespread use is leading to growing environmental problems. Plastic waste has become a major problem in the modern world [3,4]. Large amounts of plastics are released into the environment, such as soil and oceans. Plastic residues in the environment undergo interactions and thus break down into microplastics (MP) and nanoplastics (NP) through mechanical abrasion, thermal and ultraviolet (UV) decomposition, photooxidation, biodegradation, and mechanical friction [5]. Microplastics are defined as solid polymer particles with a size greater than 1 μm and less than 5000 μm and nanoplastic particles with a size of less than 100 nm. Microplastics are divided into two main groups [6]. Primary microplastic is intentionally produced and used as an additive in many products (e.g., cosmetics). It can enter the environment through wastewater. Secondary microplastics are formed by the fragmentation of larger plastic particles through hydrodynamic processes.

Regardless of their origin, microplastics and nanoplastics have become one of the most serious environmental and health problems for living organisms today. The impact of microplastics on various ecosystems such as the ocean, rivers, groundwater, wetlands, atmosphere, soil, etc., has been and is still being studied in detail [7–10]. Extensive knowledge is needed to understand the possible physical, chemical, and biological changes in the properties of microplastics and its effects on human health. Studies have reported the presence of MP particles in numerous products intended for human consumption [11,12]. Microplastic and especially nanoplastic particles can penetrate many biological barriers and possess strong toxicological properties [13]. One study investigated and confirmed that maternal lung exposure to nanopolystyrene results in translocation of plastic particles to placental and fetal tissues [14]. Mohamed Nor and colleagues found that a human can accumulate several thousand microplastic particles in the body over a lifetime [15]. On the other hand, the detection of microplastics in human feces (an average of 2 microplastic particles per g of feces) has been reported [16]. An important discovery related to the penetration of microplastics into living organisms, including mammals, was made by Ragusa and co-workers. Using Raman microspectroscopy, they detected multiple microplastic fragments in human placenta samples for the first time [17]. In recent research, plastic particles were detected in human blood [18].

Studies show that the vast majority of micro and nanoplastics found in the ecosystem consist of polyethylene (PE), polypropylene (PP),

* Corresponding authors.
E-mail addresses: ivanda@irb.hr (M. Ivanda), veres.miklos@wigner.hu (M. Veres).

https://doi.org/10.1016/j.apsusc.2022.155239
Received 16 June 2022; Received in revised form 6 October 2022; Accepted 6 October 2022
Available online 12 October 2022

polystyrene (PS), and polyethylene terephthalate (PET), which are formed by the degradation of products of these synthetic polymers [19]. The identification of plastic micro- and nanoparticles is particularly challenging due to their size. Currently, the most commonly used methods for chemical identification of microplastics are Fourier transform infrared spectroscopy (FTIR) and conventional Raman spectroscopy [20–23]. However, these two methods suffer from poor spatial resolution due to the limited diffraction resolution of the instruments. Another drawback is that Raman scattering is a weak process that limits the signal intensity. Therefore, the spatial resolution for FTIR and Raman spectroscopy is theoretically 20 μm and 1 μm, respectively [24]. Sampling, handling and identification of micro and nanoplastics is also a problem. Furthermore, these particles differ in size, color, density, and also in added additives (such as colorants and plasticizers), which makes detection even more challenging. This shows that it is not possible to effectively detect nanoplastics without further modification of the above methods.

One way to increase the sensitivity of Raman spectroscopy is to use surface-enhanced Raman spectroscopy (SERS) [25]. This robust method is widely used to identify low concentrations of numerous chemical substances such as drugs, pollutants, biomolecules, explosives, or tiny plastic particles [26–29]. The discovery of SERS in 1974 attracted much attention because of the strong enhancement of the weak Raman signal. SERS is a technique that leads to an increase in the scattering cross section for molecules adsorbed on or are in the vicinity of the metal nanostructure [30]. The higher cross section leads to an increase in the intensity of the measured Raman signal. This enhancement of the Raman signal is generally explained by electromagnetic and chemical mechanisms. The electromagnetic mechanism is explained by the enhancement of the electromagnetic field near metal surfaces due to localized surface plasmon resonance (LSPR), which occurs when the collective vibrations of the metal's valence electrons resonate with the frequency of the incident light. In the chemical mechanism, the adsorbed molecules form chemical bonds with the metal surface, and a resonance Raman scattering occurs involving these levels (the resonant Raman scattering leads to the increase of the Raman cross-section by 2–3 orders of magnitude when the energy of the incident photons is close to or equal to the energy of an electronic transition in the excited material). The amplification of the Raman signal is influenced by the choice of metal and the size and shape of the appropriate nanoparticles or nanostructures. Widely used today are colloidal solutions of silver or gold in various sizes and shapes.

An important factor that strongly influences the SERS enhancement is the aggregation (static or dynamic) of nanoparticles in the colloid. This could result in nanoparticle clusters with plasmonic properties that are different from single NPs and with plasmonic resonance wavelengths, hotspots, and enhancement efficiencies exceeding those of single NPs.

Despite the recognized advantages of the SERS method and its many potential applications, there has been relatively little literature on the use of SERS for the detection of plastic micro- or nanoparticles. Xu et al. were able to identify PS and poly(methyl methacrylate) (PMMA) microplastics down to 360 nm in size by SERS using the commercially available substrate Klarite [31]. Jeon and co-workers produced Ag nanowire network structures coated on the regenerated cellulose matrix and obtained strong SERS signals from PS nanoplastics entrapped in the network [32]. Caldwell et al. achieved detection limits of 10 μg mL^{-1} for 46 nm AuNP substrates for the 161 nm PS, 20 μg mL^{-1} for the 33 nm PS, and 15 μg mL^{-1} for the 62 nm PET [33]. The same group developed the sequential milling method for the preparation of PET particles in the nanometer range [34]. Polystyrene (PS) nanospheres can also be detected from the SERS spectrum as they pass through the single solid gold nanopore [35]. Recently, Lv et al. reported that SERS enables the detection of 100 nm sized plastics (PS) at a level as low as 40 μg mL^{-1}, distinguishing between different types of microplastic particles such as PE and PP [36]. This enhancement was achieved by aggregating silver nanoparticles (AgNPs) with salts. Last year, a study was conducted showing for the first time that when PS nanoplastics were surrounded by SERS-active silver nanoparticles (AgNPs), a series of Raman spectra with chemical information could be obtained via SERS mapping [37]. The proposed method was able to identify previously undetectable plastic particles as small as ~ 50 nm spiked in water. Recently, Hu and co-workers have developed a SERS method for detecting polystyrene nanoplastics as small as 50 nm based on a silver colloid [38]. They quantitatively analyzed four sizes of PS nanoplastics (50, 100, 200, and 500 nm) using the same SERS method but obtained different detection limits, with the highest sensitivity (detection limit of 6.25 μg mL^{-1}) obtained for 100 nm PS nanoplastics. Lee and Fang have recently developed a method where they use gold nanourchins (AuNU) as SERS substrates to detect 600 nm polystyrene particles [39]. They suggest that SERS of a single particle of PS can be induced by as few as 1–5 particles of AuNU under excitation at 785 nm.

The need for simple, inexpensive, and reproducible SERS substrates suitable for microparticle and nanoparticle detection remains strong, especially at low particle concentrations. As mentioned earlier, most studies on the use of the SERS method for the detection of micro- and nanoparticles have been performed on polystyrene particles of different sizes, likely due to their two prominent Raman bands (i.e., the ring-breathing vibrations at ≈1002 cm^{-1} and ≈1032 cm^{-1}). In this work, a sensitive and quantitative SERS method was developed for the analysis of polystyrene spheres of 350 nm, but the PE SERS signal was difficult to obtain. The developed SERS method allows detection of polystyrene microparticles at concentrations as low as 6.5 μg mL^{-1}.

2. Materials and methods

2.1. Materials

Gold(III) chloride trihydrate, trisodium citrate dihydrate, hydroxylamine hydrochloride, ascorbic acid, SDS (sodium dodecyl sulphate), sodium chloride, sodium nitrate and potassium chloride were supplied by Merck. Silver nitrate was provided by Kemika. Polystyrene spheres with diameters of 350 nm and 1 μm (2.5 % (w/v) in water) were obtained from Polysciences, Inc. (USA). Clear polyethylene microspheres (1–4 μm) in powder form were supplied by Cospheric LLC (USA). The PE dilution (200 μg mL^{-1}) was prepared in water with the addition of 1 % SDS in ultrasonic bath. High purity water (18 MΩ cm^{-1}) was used for all experiments. All chemicals were of analytical purity and were used without further preparation.

2.2. Preparation of gold nanoparticles

2.2.1. Synthesis of gold NP seeds (A1)

Au NP seeds were prepared by the little modified Turkevich method [40]. Briefly, an aqueous solution of $HAuCl_4$ (0.5 mM) was brought to a boil and the same volume of 1.7 mM sodium citrate was added. The solution was stirred for 15 min and then cooled to room temperature with stirring.

2.2.2. Synthesis of gold NPs (sample A2)

1 mL of the previously prepared gold nanoparticle seed (A1) was added to 9 mL of water, followed by the addition of 0.1 mL of 0.2 M $NH_2OH{\cdot}HCl$. The mixture was stirred vigorously, and 0.084 mL of 25.4 mM $HAuCl_4{\cdot}3\ H_2O$ was added.

2.2.3. Synthesis of gold NPs (sample A3)

The procedure described above was repeated, but sample A2 was used as a seed solution.

2.2.4. Synthesis of gold NPs (sample A4)

The seed solution was prepared by adding 100 μL of 10 mM $HAuCl_4$ and 100 μL of 10 mM $AgNO_3$ to 5 mL of 10 mM ascorbic acid solution.

The reaction mixture was vigorously stirred for 15 s and then 5 mL of 3 mM $HAuCl_4 \cdot 3\ H_2O$ was added. The reaction mixture was vigorously stirred for another 60 s. Finally, 1 mL of 20 mM sodium citrate solution was added to stabilize the mixture.

2.2.5. Synthesis of gold NPs (sample A5)

Au NPs were synthesised according to the slightly modified Pollitt protocol [41]. A solution of 0.5 mL gold(III) chloride trihydrate (24 mM) and 50 mL of ultrapure water was heated to 150 °C with vigorous stirring. During the boiling, 6 mL of 39 mM sodium citrate dihydrate was added. After 2 min, another 4.2 mL of gold(III) chloride trihydrate (24 mM) was added to stimulate particle growth. Within a few minutes, the colour of the solution changed from transparent to black and finally to deep red. The solution was allowed to cool with constant stirring. All gold colloids were stored at 8 °C in the dark until further use.

2.3. Preparation of SERS samples

In a small glass tube, 500 µL of Au NPs, 25 µL of microplastic solution, and 25 µL of aggregating agent were added unless otherwise indicated. The solution was vortexed and 2 µL of the droplet containing the plastic particles, gold nanoparticles, and aggregating agent was placed on a silicon or glass wafer coated with gold. The sample was covered until it dried in air at room temperature. After the droplet evaporated, Raman spectra were recorded. The sample preparation procedure is shown in Fig. 1.

2.4. Characterization of nanoparticles

The size and size distribution of gold nanoparticles were studied using a UV–vis spectrometer (Cary, Agilent) and a scanning electron microscope (SEM) (Mira-3, Tescan). SEM images were acquired at different magnifications with an accelerating voltage of 5 kV to avoid charging or damaging the sample. ImageJ software was used for SEM analysis and determination of particle size distribution. Dynamic light scattering (DLS) was used to further evaluate the diameter distribution. DLS measurements were performed using the Zetasizer Nano S, while zeta potential studies were performed using the Zetasizer Nano Z (Malvern). Size distributions were reported as distributions by intensity, and results are presented as the mean of at least 3 measurements. Zeta potential was reported as the mean of three measurements. Raman spectra were recorded using a Renishaw 1000 micro-Raman spectrometer connected to a Leica DM/LM microscope. The excitation source was a diode laser with a wavelength of 785 nm focused on a spot of 1.5 µm diameter on the sample surface. Raman spectra were also recorded using a Renishaw inVia micro-Raman spectrometer connected to a Leica microscope. A 632 nm diode laser was used as the excitation source, and the laser beam was focused on a spot 1–2 µm in diameter on the sample surface using a 50 × magnification objective. The laser excitation power on the sample was about 5 mW. The 520 cm^{-1} Raman band of a silicon wafer a was used to calibrate the spectrometer. The measurement time for each sample was 10 s with 5 accumulations unless otherwise indicated. Raman measurements were made at several locations on the substrate surface, and the measurement was repeated at the spot where the SERS signal was highest.

3. Results and discussion

3.1. Characterization of gold nanoparticles

Au colloids with different particle sizes were synthesized and studied to determine the influence of the diameter of NP on the performance of SERS spectra. The synthesized colloidal gold solutions were characterized by different techniques, the first of which is absorption spectroscopy. Fig. 2 shows the UV–vis absorption spectra of the synthesized gold NP with plasmon bands between 519 and 546 nm, as expected for spherical Au NPs in the size range of 20 to 100 nm. Samples A2, A3, A4 and A5 have the absorption maximum at 528, 546, 534 and 533 nm, respectively (Table 1). Samples A4 and A5 have the smallest FWHM value of the absorption peak, indicating a narrow size distribution.

SEM measurements were performed to observe the size and morphology of the synthesized Au NPs (Fig. 3). Samples A2 and A3 consist of fairly uniform spherical nanoparticles. Sample A4, on the other hand, exhibits an uneven surface characterized by the presence of spikes on the surface. Samples A2, A3 and A4 have an average particle diameter of 33.2, 67.5, and 93.7 nm, respectively. In sample A5, the

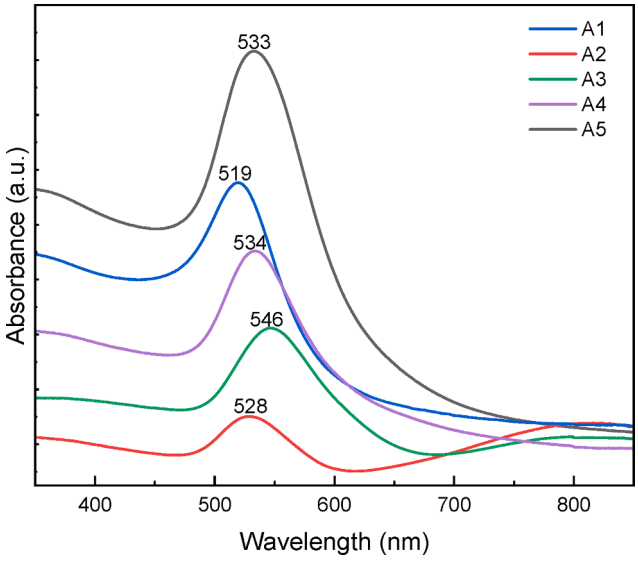

Fig. 2. UV–vis spectra of synthesized gold nanoparticles.

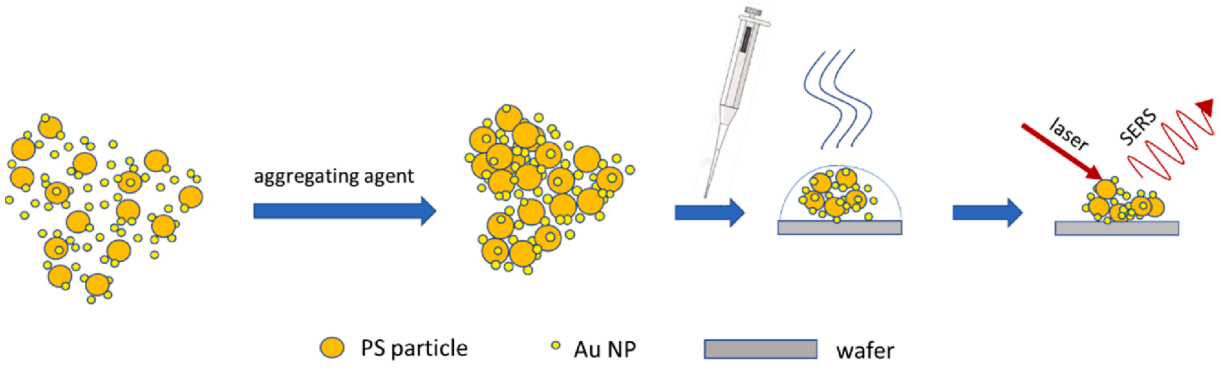

Fig. 1. Schematic diagram of PS analysis using the SERS method.

Table 1
The characterization of the prepared samples.

Sample	Zeta potential (ζ) (mV)	Hydrodynamic diameter[a] (nm)	λ^{max} (nm)	D_{SEM} (nm)	Number of Au NPs[b] (mL^{-1})	Surface area of Au NPs[c] (m^2/L)
A2	−19.8	106.7 (88.3 %)	528	32.21 ± 3.92	1.45×10^{13}	47.1
A3	−29.1	402.6 (90.6 %)	546	67.51 ± 6.35	1.61×10^{11}	2.4
A4	−38.5	208.5 (85.2 %)	534	93.73 ± 12.54	2.94×10^{10}	0.9
A5	−35.7	48.9 (60.3 %)	533	(23.53 ± 3.55) × (35.48 ± 5.07)	1.34×10^{12}	3.8

[a] Percentages in parentheses indicate percentage based on intensity distributions.
[b] The number of Au NPs in the colloid was estimated by dividing the total mass of gold in $HAuCl_4$ used to synthesize the gold NPs by the individual mass of a gold NP.
[c] The surface area of the Au NPs was calculated assuming that all NPs were spherical.

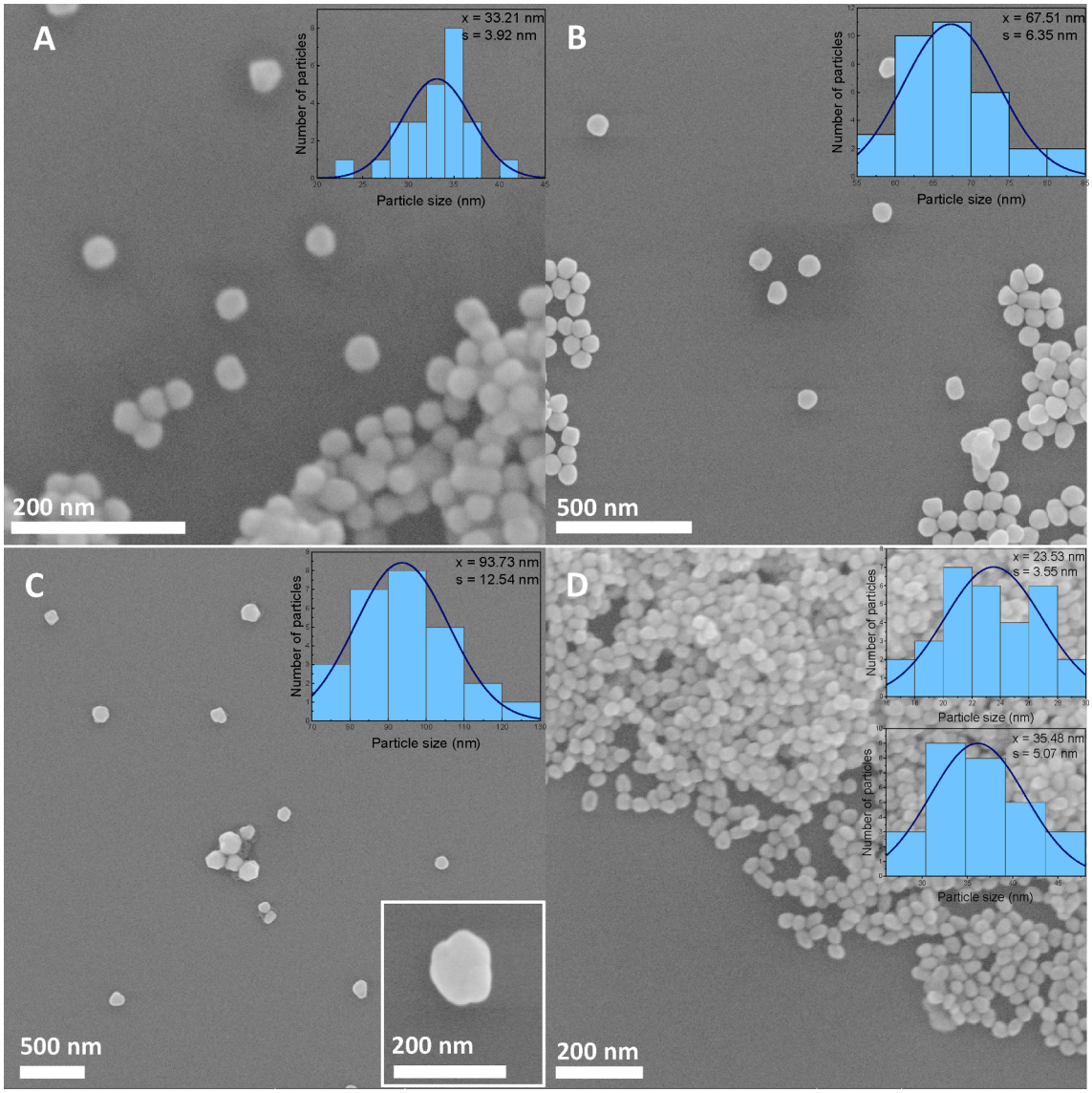

Fig. 3. SEM images of synthesized gold nanoparticles: a) A2, b) A3, c) A4 (inset: a single gold NP) and d) A5. The insets show the particle size distributions.

shape of the particles is mainly elliptical (or nanorod) with an approximate axial ratio of 23.5 × 35.5 nm (Fig. 3d). The hydrodynamic size distributions by intensity for the colloidal gold samples are listed in Table 1. The dynamic light scattering (DLS) measurements revealed that the hydrodynamic diameter of the Au NPs is slightly larger than the size estimated by SEM. There are systematic differences between these two methods due to the coating material and the solvent layer adhering to the nanoparticles, which affect the larger hydrodynamic radius. The zeta potential (ζ) measurements (Table 1) indicate negatively charged, stable particles that do not tend to aggregate spontaneously.

After determining the average size of the gold NPs using SEM, the number of Au NPs in the colloidal solutions and their surface area were calculated, assuming that the gold is completely reduced [42]. The number of Au NPs was estimated by calculating the volume of gold used in the reaction and the average volume of NP. The surface area of Au NPs was simply calculated using the formula for the surface area of a sphere

and multiplied by the calculated number of nanoparticles (Table 1).

3.2. Raman and SERS measurements

3.2.1. Detection of polystyrene

The gold colloids have a plasmon maximum at about 520 nm, and one would expect efficient excitation at 488 nm or 532 nm to be used for SERS. However, because of the formation of aggregates of Au nanoparticles required for SERS, which shift the plasmon resonance toward red, excitation at 785 nm was used, which is more favourable. Prior to the SERS measurements, the Raman spectra of the PS350 and PS1000 spheres were recorded by drop-casting the stock solutions onto a clean Si wafer (Fig. 4). The two prominent PS peaks are at 1004 cm^{-1}, which is a result of ring breathing vibration, and at 1032 cm^{-1}, which is a result of C—H in-plane deformation [43]. The Raman bands in the range 1150 to 1200 cm^{-1} are also observed (C—C stretches), as well as the ring skeletal stretch at 1605 cm^{-1}. While the intensity is good for the 1 μm PS spheres, the intensity of the Raman signal is greatly reduced for the 350 nm spheres, so that not even the two most intense bands at 1005 and 1034 cm^{-1} can be distinguished and only bands originating from the Si wafer can be seen (2nd order of Si at ≈ 950 cm^{-1}) (Fig. 4). Based on previous studies, the representative Raman signal at 1005 cm^{-1} was selected to further identify the PS350 SERS signal [44]. There is no clear way to describe how SERS enhancement scales with the size of the analyte. The most important factors affecting enhancement are the distance of the analyte from the substrate, its uniform distribution and aggregation. This means that it is important to optimize the SERS method for each size of PS (or PE) sphere. The size of the PS particles we studied was much larger than the size of the gold nanoparticles, leading to the conclusion that the enhancement is mainly due to the electric field enhancement by the Au nanoparticles and their aggregates attached to the surface of the PS sphere.

The results of many studies show that the improvement of SERS depends largely on many factors including the size and concentration of gold NPs [42]. The influence of colloids prepared by different synthesis methods (and correspondingly different sizes and concentrations of Au NPs) on the PS350 SERS signal was investigated and compared by using colloids A2, A3, A4 and A5 with the same colloid volume (Fig. 5a). The PS concentration used to determine the best Au colloid, the appropriate ratio of colloid to PS350 volume, and the aggregating agent was 100 μg mL^{-1}. The use of colloid A5 gave the best band intensity (by height) at 1005 cm^{-1}, but good intensity was also obtained with sample A2. Samples A3 and A4 had slightly lower intensity at 1005 cm^{-1}, but the band at 1032 cm^{-1} was better visible. These results show that it is better to use smaller particles (≈35 nm) in high concentration to obtain a good SERS signal. The higher number of Au NPs can cause a better coverage of the polystyrene surface and increases the number of hot spots, resulting in a larger enhancement. Increasing the Au particle size from 32 to 94 nm resulted in a lower PS350 SERS signal (Fig. 5a). The reason is probably the decreasing surface density of the particles with increasing Au NPs size. As the Au NP size increases, the final PS350 particle coverage decreases, reducing the number of hot spots in the excitation region of SERS and thus reducing the signal. Additionally, since the aggregation of the Au NPs contributes also to the SERS enhancement, larger particles might form clusters whose plasmonic properties do not efficiently support the SERS process.

The optical properties of metal nanostructures depend more on shape than size. Spherical Au nanoparticles have only one dipolar plasmon resonance, while complex structures typically have multiple dipole modes leading to broad plasmon absorption spectra. The induced electronic cloud on complex structures is not homogeneously distributed on the surface. This could explain the better enhancement when Au nanorods (sample A5) are used as SERS substrates compared to enhancement by spherical Au NPs. Due to the highest intensity, sample A5 was selected for further work.

To determine the appropriate colloid volume for analysis of PS350, different volume ratios between the A5 colloid and PS350 were tested, ranging from 10:1 to 60:1 (Fig. 5b). The intensity increases when the volume ratio of colloid to PS is changed from 10:1 to 20:1, but there is not much difference between the ratios of 20:1, 40:1, or 60:1 colloid to

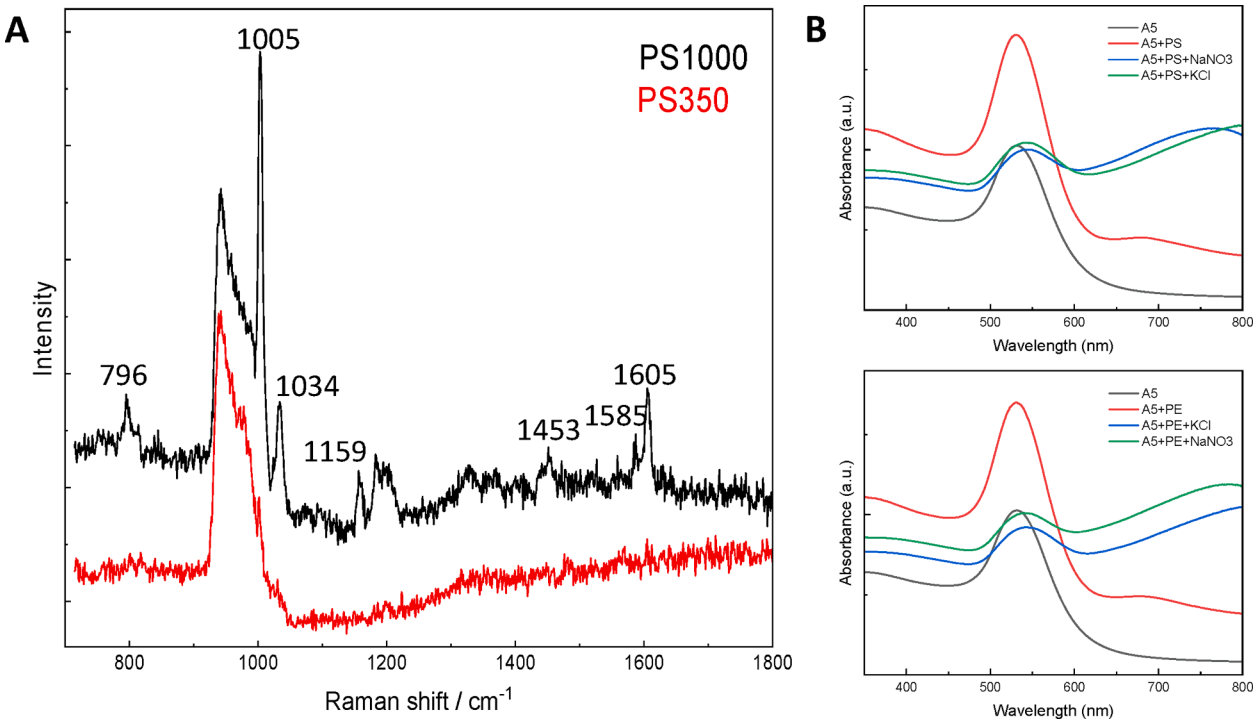

Fig. 4. Raman spectra of 350 nm polystyrene spheres (PS350) (red) and 1000 nm polystyrene spheres (PS1000) (black), both 25 mg mL^{-1} on Si wafer (not baseline corrected); b) UV–vis spectra of Au NPs solution and their mixtures with PS350 or PE and KCl or $NaNO_3$ (0.6 M) solution. (For interpretation of the references to color in this figure legend, the reader is referred to the web version of this article.)

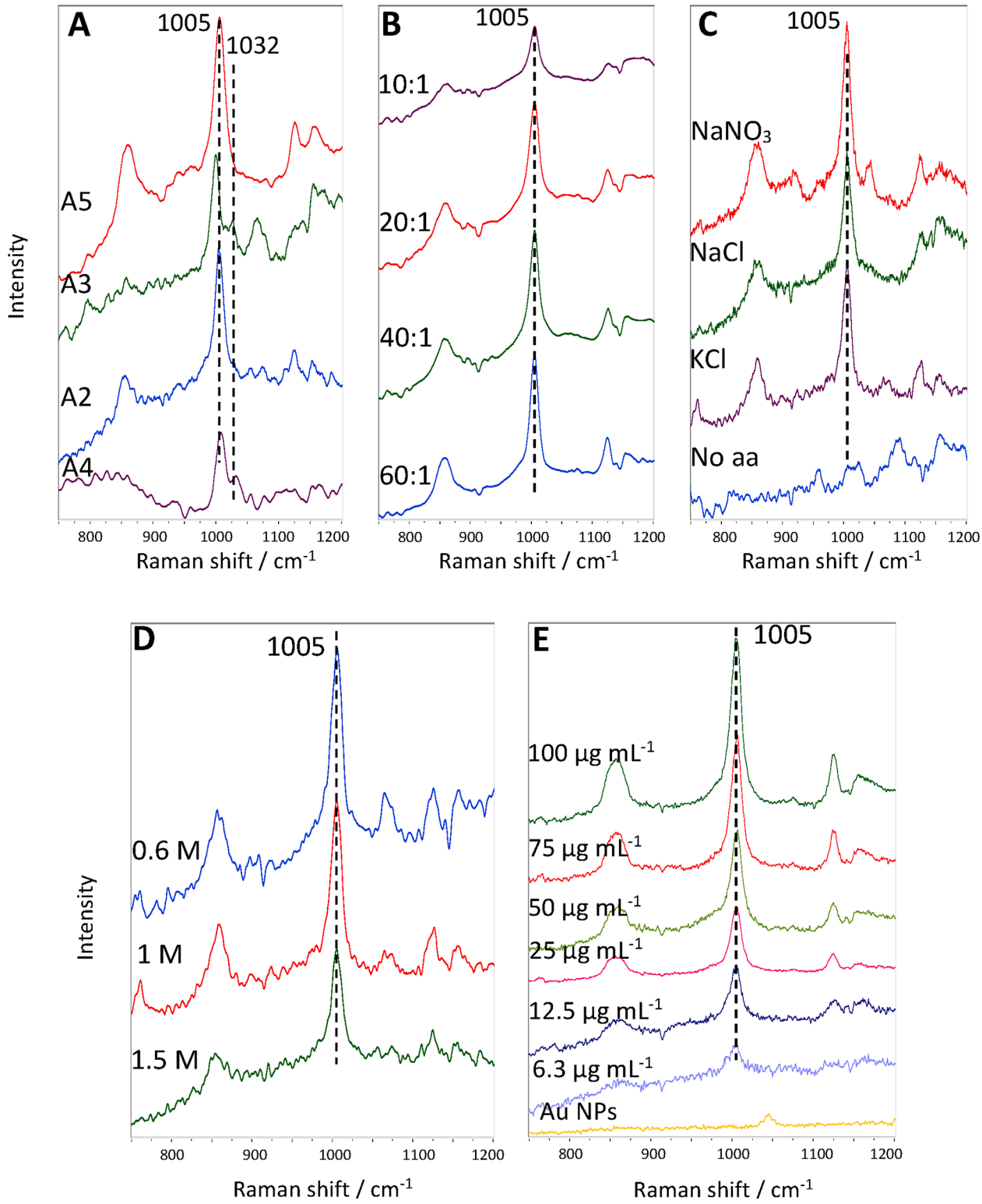

Fig. 5. SERS spectra of PS350 with different: a) Au colloids, b) volume ratios of Au NPs/PS350 solutions, c) aggregating agents, d) KCl concentrations and e) concentrations (100, 75, 50, 25, 12.5 and 6.25 µg mL^{-1}). The concentration of PS350 was 100 µg mL^{-1} and concentrations of aggregating agents (aa) were 1 M if not stated differently.

PS spheres. When the amount of colloid is increased beyond a certain volume, the signal is not further enhanced. As will be discussed later, the PS350 particles are well covered with Au NPs even with a lower amount of colloid solution.

Hu and co-workers, in a recent paper emphasized the role of aggregating agent in the quantitative analysis of polystyrene (PS) nanoplastics using silver colloid [41]. In our case, the detection of PS350 was greatly facilitated by the use of aggregating agents. The SERS spectra of PS350 were determined by adding 1 M $NaNO_3$, NaCl and KCl to the A5 gold colloid to find the optimal aggregating agent. Fig. 5c shows the SERS signal intensity of PS350 when different aggregating agents were used. The intensity was significantly increased when any of the salts were

added to the sample, so any of the salts tested could be used. The negligible differences in the SERS spectra of PS350 when different salts were added to the colloids may be due to both the degree of aggregation of the colloids and changes in the surface area of the gold structures. Two other KCl concentrations (0.6 and 1.5 M) were tested, and the best SERS signal enhancement was obtained for a concentration of 0.6 M (Fig. 5d), which was used for the further experiments. An additional experiment was performed to test whether the addition of PS350 and PE itself had any effect on colloid aggregation. Fig. 4b shows the UV–vis absorption spectra for the A5 colloid with the addition of PS350 and the aggregating agent. It can be seen that there is no shift in the absorption maximum when only PS350 or PE spheres are added to the A5 colloid. Only after the addition of KCl or $NaNO_3$ does another absorption maximum appear at higher wavelengths, indicating the formation of aggregates.

PS350 solutions with concentrations of 6.25, 12.5, 25, 50, 75 and 100 μg mL^{-1} were studied to test the quantitative capability of the developed SERS method. Fig. 5e shows the SERS spectra of the different PS350 concentrations. A clear PS SERS peak at 1005 cm^{-1} was observed for all concentrations. As the concentration decreases, the intensity of the band decreases and it is visible up to a concentration of 6.25 μg mL^{-1}, so this concentration was taken as the limit of detection (LOD) for the developed SERS method. This LOD is comparable to the data published for silver NPs [38].

3.2.1.1. Detection of polyethylene. Fig. 6a shows the Raman spectrum of polyethylene (PE) powder obtained with 632 nm laser excitation. The most intensive peaks are 1291 cm^{-1} (CH_2 twisting mode), 1127 cm^{-1} (symmetric C—C stretching mode) and 1060 cm^{-1} (the anti-symmetric C—C stretching mode) [45]. Three distinct peaks around 1400 cm^{-1} are assigned to the CH_2 bending modes, while the peaks at 2838 and 2871 cm^{-1} are assigned to the symmetric and asymmetric CH_2 stretching modes, respectively [46].

The SERS signal from the PE spheres was difficult to obtain. Of the various measurements, only several showed a satisfactory result (Fig. 6b). Obtaining a good spectrum was not improved by changing the colloid or adding an aggregating agent. Fig. 6c shows the SEM image of polyethylene spheres mixed with a gold A5 colloid. It can be seen that none of the spheres are covered with gold and that the Au nanoparticles are only found in the small area where the spheres touch. This situation did not change even after the addition of the aggregating agent. This could be a possible reason for the difficulty in obtaining the SERS spectrum. In contrast, the surface of the PS350 spheres was almost completely covered with gold nanoparticles (Fig. 6d). Since the coverage of the PE microspheres with Au nanoparticles varies from sphere to sphere, it is difficult under the Raman microscope to find sites with suitable SERS signal. One possible way to overcome this weakness is to improve the coverage of the PE particles with gold NPs, which will be the goal of further investigations.

4. Conclusions

Due to the large occurrence of micro- and nano-sized plastic particles in the environment today, there is an increasing need for a fast and efficient analysis of these particles, and the SERS method has so far proven to be a convenient, rapid, and simple method for the detection of many chemicals. The choice of metal used as the SERS substrate affects signal enhancement. Previously, it was discussed that Ag is a superior

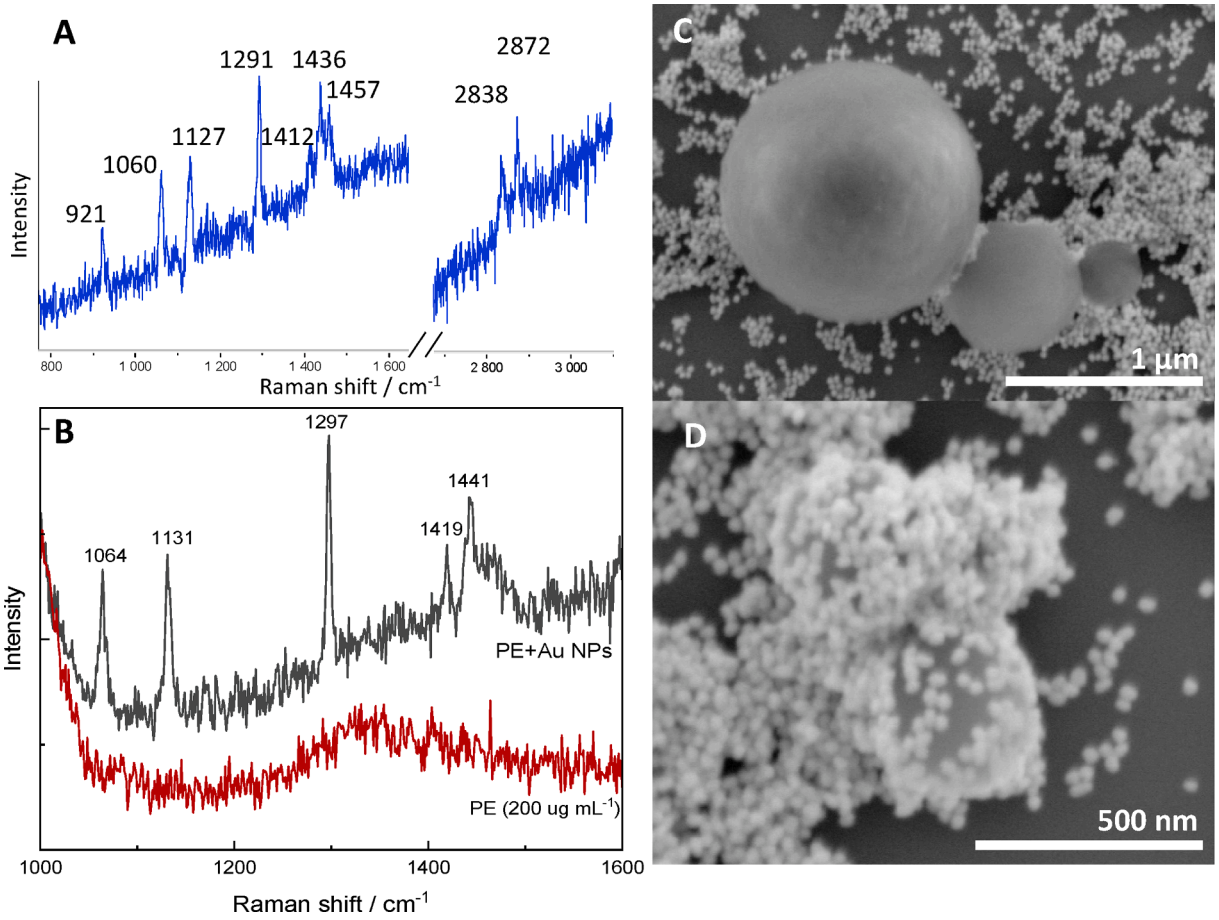

Fig. 6. a) Raman spectra of polyethylene (PE) powder - spheres with a diameter of 1–4 μm, excitation 632 nm, b) SERS spectra of PE (200 μg mL^{-1}) with Au colloid (A2) without aggregating agent, excitation 785 nm, not baseline corrected, c) SEM image of PE with A5 colloid, d) SEM image of PS with A5 colloid.

material for SERS detection of polystyrene. Therefore, it was challenging to use gold, but its advantages over silver (such as oxidation resistance, biocompatibility, etc.) are numerous.

In this work, a method for detecting 350 nm polystyrene spheres using gold colloids was developed. Gold nanoparticles (Au NPs) of four different sizes were synthesized, characterized, and used as SERS active substrate for microplastic detection. The calculated mean particle size from SEM analysis was estimated to be 33.2, 67.5 and 93.7 nm for spherical samples. The gold nanorod sample has an approximate particle size of 23.5 × 35.5 nm. The influence of different sizes and concentrations of Au NPs on the PS350 SERS signal was investigated, and the nanorod colloid gave the best intensity at 1005 cm^{-1} and was therefore selected for further work. After the best parameters for the nanorod colloid were determined experimentally, the detection limit of 6.25 μg mL^{-1} was demonstrated, making this method sensitive enough for quantitative analysis. The method developed in this work is suitable for the detection of polystyrene in aqueous solutions.

CRediT authorship contribution statement

L. Mikac: Conceptualization, Methodology, Investigation, Formal analysis, Data curation, Visualization, Writing – original draft. **I. Rigó:** Formal analysis, Investigation. **L. Himics:** Formal analysis, Investigation. **A. Tolić:** Investigation. **M. Ivanda:** Resources, Supervision. **M. Veres:** Resources, Supervision.

Declaration of Competing Interest

The authors declare that they have no known competing financial interests or personal relationships that could have appeared to influence the work reported in this paper.

Data availability

Data will be made available on request.

Acknowledgements

This work was supported by project no. 2018-1.2.1-NKP-2018-00012 which has been implemented with the support provided from the National Research, Development and Innovation Fund of Hungary, financed under the 2018-1.2.1-NKP funding scheme. The research was partially supported by the project co-financed by the Croatian Government and the European Union through the European Regional Development Fund - Competitiveness and Cohesion Operational Programme (KK.01.1.1.01.0001). This work was supported in part by the Foundation of the Croatian Academy of Sciences and Arts and by the National Research, Development and Innovation Office – NKFI, OTKA PD-134625 grant, as well as by the 2018-2.1.12-TET-HR-2018-00003 Croatian-Hungarian bilateral S&T project.

References

[1] R.C. Thompson, et al., Plastics, the environment and human health: Current consensus and future trends, Philos. Trans. R. Soc. B: Biol. Sci. 364 (1526) (2009) 2153–2166.
[2] R.C. Thompson, et al., Our plastic age, Philos. Trans. R. Soc. B: Biol. Sci. 364 (1526) (2009) 1973–1976.
[3] E.J. North, R.U. Halden, Plastics and environmental health: The road ahead, Rev. Environ. Health 28 (1) (2013) 1–8.
[4] F. Gu, et al., From waste plastics to industrial raw materials: A life cycle assessment of mechanical plastic recycling practice based on a real-world case study, Sci. Total Environ. 601–602 (2017) 1192–1207.
[5] R. Kumar, et al., Effect of physical characteristics and hydrodynamic conditions on transport and deposition of microplastics in riverine ecosystem, Water 13 (19) (2021) 2710.
[6] W.M. Wu, J. Yang, C.S. Criddle, Microplastics pollution and reduction strategies, Front. Environ. Sci. Eng. 11 (1) (2017).
[7] J.K.H. Wong, et al., Microplastics in the freshwater and terrestrial environments: Prevalence, fates, impacts and sustainable solutions, Sci. Total Environ. 719 (2020).
[8] C. Edo, et al., Fate of microplastics in wastewater treatment plants and their environmental dispersion with effluent and sludge, Environ. Pollut. 259 (2020).
[9] H.S. Auta, C.U. Emenike, S.H. Fauziah, Distribution and importance of microplastics in the marine environmentA review of the sources, fate, effects, and potential solutions, Environ. Int. 102 (2017) 165–176.
[10] A. Facciolà, et al., Newly emerging airborne pollutants: Current knowledge of health impact of micro and nanoplastics, Int. J. Environ. Res. Public Health 18 (6) (2021) 1–17.
[11] J.H. Kwon, et al., Microplastics in food: a review on analytical methods and challenges, Int. J. Environ. Res. Public Health 17 (18) (2020) 1–23.
[12] H. Bouwmeester, P.C.H. Hollman, R.J.B. Peters, Potential health impact of environmentally released micro- and nanoplastics in the human food production chain: experiences from nanotoxicology, Environ. Sci. Technol. 49 (15) (2015) 8932–8947.
[13] M. Xu, et al., Internalization and toxicity: a preliminary study of effects of nanoplastic particles on human lung epithelial cell, Sci. Total Environ. 694 (2019).
[14] S.B. Fournier, et al., Nanopolystyrene translocation and fetal deposition after acute lung exposure during late-stage pregnancy, Part. Fibre Toxicol. 17 (1) (2020) 55.
[15] N.H. Mohamed Nor, et al., Lifetime accumulation of microplastic in children and adults, Environ. Sci. Technol. 55 (8) (2021) 5084–5096.
[16] Detection of various microplastics in human stool, Ann. Internal Med. 171 (7) (2019) 453–457.
[17] A. Ragusa, et al., Plasticenta: first evidence of microplastics in human placenta, Environ. Int. 146 (2021), 106274.
[18] H.A. Leslie, et al., Discovery and quantification of plastic particle pollution in human blood, Environ. Int. (2022), 107199.
[19] A. Käppler, et al., Identification of microplastics by FTIR and Raman microscopy: a novel silicon filter substrate opens the important spectral range below 1300 cm−1 for FTIR transmission measurements, Anal. Bioanal. Chem. 407 (22) (2015).
[20] M. Kedzierski, et al., A machine learning algorithm for high throughput identification of FTIR spectra: application on microplastics collected in the Mediterranean Sea, Chemosphere 234 (2019) 242–251.
[21] V. Morgado, et al., Validated spreadsheet for the identification of PE, PET, PP and PS microplastics by micro-ATR-FTIR spectra with known uncertainty, Talanta 234 (2021).
[22] B.N. Vinay Kumar, et al., Analysis of microplastics of a broad size range in commercially important mussels by combining FTIR and Raman spectroscopy approaches, Environ. Pollut. 269 (2021).
[23] J. Li, H. Liu, J. Paul Chen, Microplastics in freshwater systems: a review on occurrence, environmental effects, and methods for microplastics detection, Water Res. 137 (2018) 362–374.
[24] V. Nava, M.L. Frezzotti, B. Leoni, Raman spectroscopy for the analysis of microplastics in aquatic systems, Appl. Spectrosc. 75 (11) (2021) 1341–1357.
[25] P.L. Stiles, et al., Surface-enhanced Raman spectroscopy, Annu. Rev. Anal. Chem. 1 (1) (2008) 601–626.
[26] Y. Wang, B. Yan, L. Chen, SERS tags: novel optical nanoprobes for bioanalysis, Chem. Rev. 113 (3) (2013) 1391–1428.
[27] S. Pang, T. Yang, L. He, Review of surface enhanced Raman spectroscopic (SERS) detection of synthetic chemical pesticides, TrAC - Trends Anal. Chem. 85 (2016) 73–82.
[28] T. Jančı, et al., Determination of histamine in fish by Surface Enhanced Raman Spectroscopy using silver colloid SERS substrates, Food Chem. 224 (2017) 48–54.
[29] A. Hakonen, et al., Explosive and chemical threat detection by surface-enhanced Raman scattering: a review, Anal. Chim. Acta 893 (2015) 1–13.
[30] J. Langer, et al., Present and future of surface-enhanced Raman scattering, ACS Nano 14 (1) (2020) 28–117.
[31] G. Xu, et al., Surface-enhanced Raman spectroscopy facilitates the detection of microplastics <1 μm in the environment, Environ. Sci. Technol. 54 (24) (2020) 15594–15603.
[32] Y. Jeon, et al., Detection of nanoplastics based on surface-enhanced Raman scattering with silver nanowire arrays on regenerated cellulose films, Carbohydr. Polym. 272 (2021).
[33] J. Caldwell, et al., Detection of sub-micro- and nanoplastic particles on gold nanoparticle-based substrates through surface-enhanced Raman scattering (Sers) spectroscopy, Nanomaterials 11 (5) (2021).
[34] J. Caldwell, et al., Fluorescent plastic nanoparticles to track their interaction and fate in physiological environments, Environ. Sci. Nano 8 (2) (2021) 502–513.
[35] X.-L. Nie, et al., Recognition of plastic nanoparticles using a single gold nanopore fabricated at the tip of a glass nanopipette, Chem. Commun. 55 (45) (2019) 6397–6400.
[36] L. Lv, et al., In situ surface-enhanced Raman spectroscopy for detecting microplastics and nanoplastics in aquatic environments, Sci. Total Environ. 728 (2020), 138449.
[37] X.X. Zhou, et al., Identification of polystyrene nanoplastics using surface enhanced Raman spectroscopy, Talanta 221 (2021).
[38] R. Hu, et al., Quantitative and sensitive analysis of polystyrene nanoplastics down to 50 nm by surface-enhanced Raman spectroscopy in water, J. Hazard. Mater. 429 (2022), 128388.
[39] C.-H. Lee, J.-K.-H. Fang, The onset of surface-enhanced Raman scattering for single-particle detection of submicroplastics, J. Environ. Sci. 121 (2022) 58–64.
[40] J. Turkevich, P.C. Stevenson, J. Hillier, A study of the nucleation and growth processes in the synthesis of colloidal gold, Discuss. Faraday Soc. 11 (1951) 55–75.

[41] M.J. Pollitt, et al., Measuring antibody coatings on gold nanoparticles by optical spectroscopy, RSC Adv. 5 (31) (2015) 24521–24527.
[42] S. Hong, X. Li, Optimal size of gold nanoparticles for surface-enhanced Raman spectroscopy under different conditions, J. Nanomater. 2013 (2013), 790323.
[43] M. Mazilu, et al., Optimal algorithm for fluorescence suppression of modulated Raman spectroscopy, Opt. Express 18 (2010) 11382–11395.
[44] Y. Jeon, et al., Detection of nanoplastics based on surface-enhanced Raman scattering with silver nanowire arrays on regenerated cellulose films, Carbohydr. Polym. 272 (2021), 118470.
[45] T. Kida, Y. Hiejima, K.-H. Nitta, Raman spectroscopic study of high-density polyethylene during tensile deformation, Int. J. Exp. Spectrosc. Tech. 1 (2016) 1–6.
[46] M. Bredács, et al., Prediction of polyethylene density from FTIR and Raman spectroscopy using multivariate data analysis, Polym. Test. 104 (2021), 107406.